

Electrochemical and spectroelectrochemical properties of novel lutetium(III) mono- and bis-phthalocyanines



Mürsel Arıcı^a, Ceyda Bozoğlu^b, Ali Erdoğmuş^c, Ahmet Lütfi Uğur^d, Atif Koca^{b,*}

^a Eskisehir Osmangazi University, Faculty of Arts and Sciences, Department of Chemistry, 26480 Eskisehir, Turkey

^b Department of Chemical Engineering, Faculty of Engineering, Marmara University, Göztepe, 34722 Istanbul, Turkey

^c Department of Chemistry, Yıldız Technical University, Esenler, 34210 Istanbul, Turkey

^d Yenice Vocational School, Çanakkale 18 March University, Yenice/Çanakkale, Turkey

ARTICLE INFO

Article history:

Received 14 May 2013

Received in revised form 26 August 2013

Accepted 11 September 2013

Available online 11 October 2013

Keywords:

Electrochemistry, Lutetium

Bis-phthalocyanines

Spectroelectrochemistry

Electrocolorimetry

Electrochromism

ABSTRACT

Peripherally and non-peripherally substituted mono and sandwich lutetium(III) phthalocyanines bearing 3,4-(dimethoxyphenylthio) substituents have been synthesized and characterized by elemental analysis, FT-IR, UV-vis spectroscopy and mass spectroscopy. Voltammetric, *in-situ* spectroelectrochemical, and *in-situ* electrocolorimetric characterization of the newly synthesized phthalocyanines were performed in solution. Changing the number and the position the substituents altered the reversibility of the electron transfer processes and affected the easy of electron transfer reactions. While the mono phthalocyanines had an oxidation-reduction peak separation ($\Delta E_{1/2}$) higher than 1.50 V, this value decreased up to 0.36 V due to the $\pi-\pi$ interaction of phthalocyanine rings around the lutetium core. Solvent of the electrolytic system also affected the redox behaviors of the complexes considerably. *In-situ* electrocolorimetric method was applied to investigate the color of the electrogenerated anionic and cationic forms of the complexes for their possible electrochromic applications.

© 2013 Elsevier Ltd. All rights reserved.

1. Introduction

For designing new devices for electrochemical applications, metallophthalocyanines (MPcs) have extensively studied because of their properties such as electrochromic [1–3], semiconductor [4], liquid crystal material [5], electrosensor [6–9], and electrocatalytic behaviors [10–12]. Among phthalocyanine derivatives, the syntheses of lanthanide(III) phthalocyanines have attracted great attention due to their physical, electrical, optical, and electrochemical properties originated from their extensive π -electron delocalization and their thermal and chemical stability [13–15]. Lanthanide(III) phthalocyanines, especially lutetium phthalocyanines have been investigated owing to their electrochromic and gas sensing properties and high intrinsic conductivity [1,16–18]. It is well documented that these properties can be tuned by changing the electron-donating or electron-withdrawing substituents on the phthalocyanine ring [15,19–22].

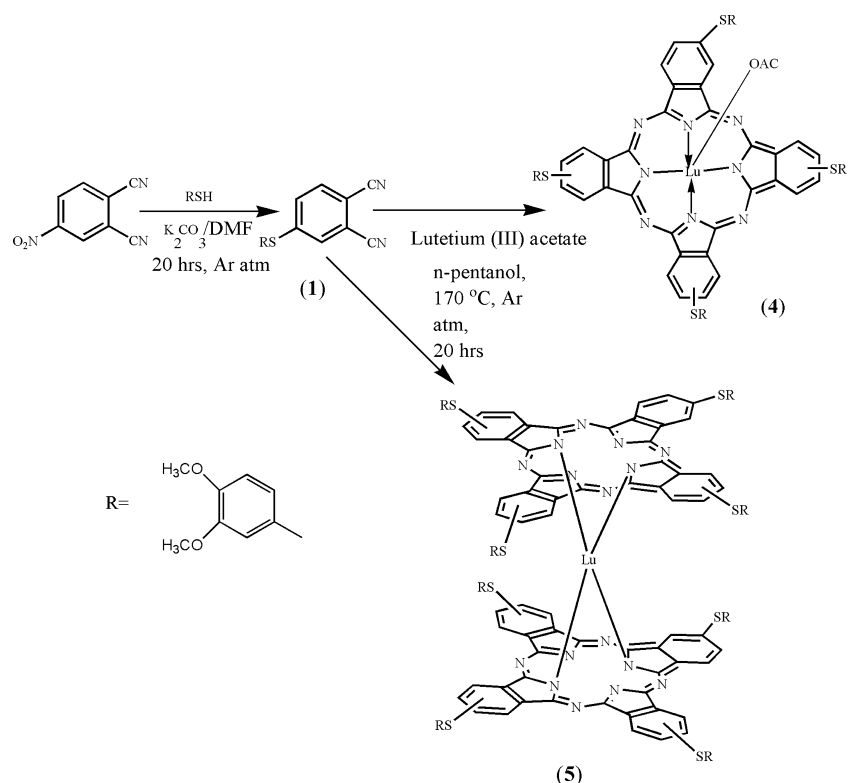
The specific electronic structure, characterized by the presence of an intramolecular axial interaction between the ligand π systems, allows sandwich complexes to find application in modern high-technology fields. Structural control of their

properties is possible by varying the nature of the central metal ion and the substituents on the phthalocyanine rings. The electronic and steric effects of substituents can influence the orbital and molecular structure of the MPc complexes, and thus affect intrinsic physicochemical properties. MPcs complexes that are peripherally or non-peripherally substituted with alkanethiol and phenylthiol derivatives showed rich electrochemical and photochemical properties [23–25]. Moreover, the presence of electron donating sulphur groups on Pc caused shifting of the Q-band to the longer wavelengths, which directly alter the electrochemical responses [25–27]. In this respect, it needs to understand the electrochemical and spectroelectrochemical properties of the newly synthesized complexes to open a way to their technological applications.

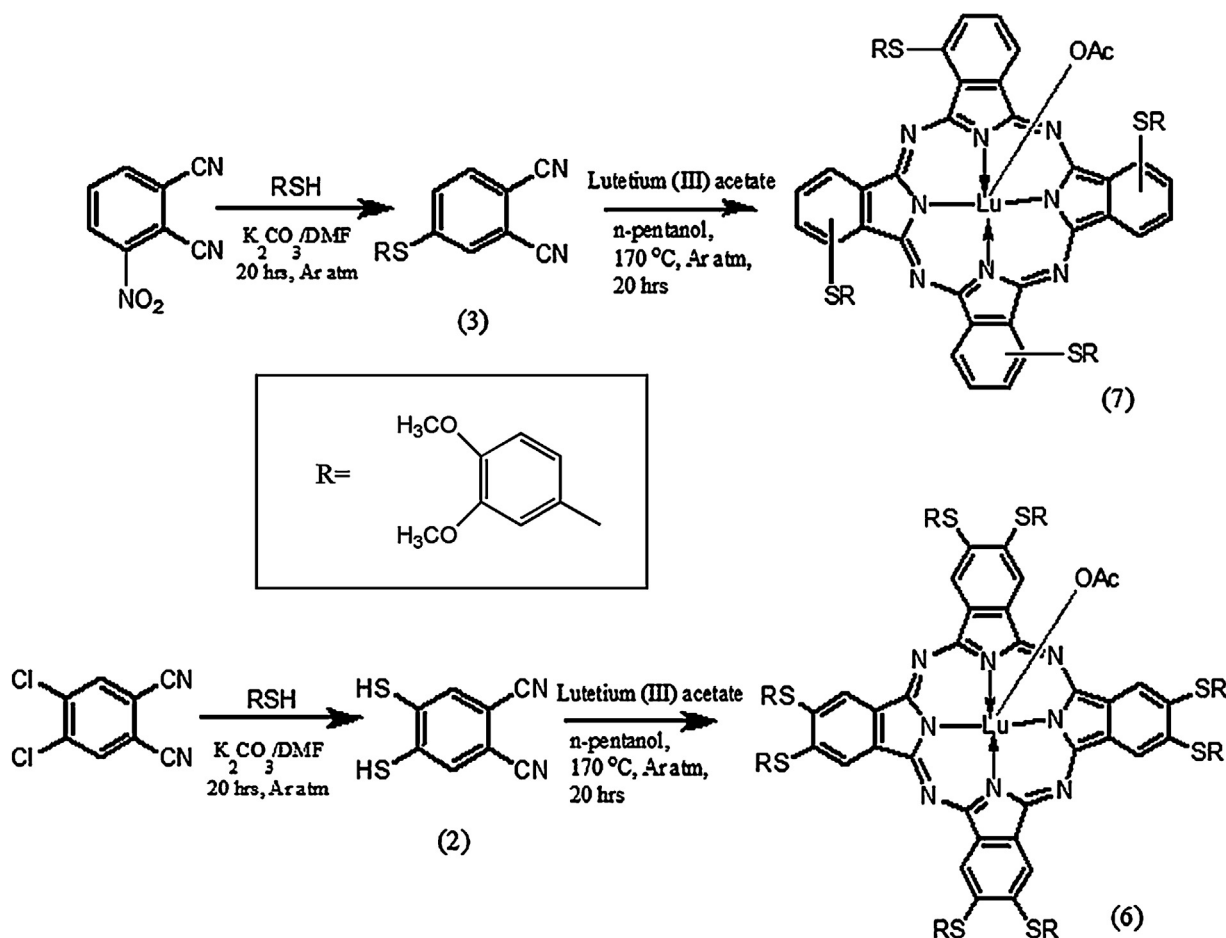
It is well known that extent electrochemical properties of sandwich phthalocyanines determine their possible technological applications [15]. Although mono and bis phthalocyanines have frequently been described, comparison of those bearing different number of substituents at different positions have not been extensively studied, especially those bearing tetra and octa substituents. Thus in this study, we have synthesized and reported the spectroscopic characterization and voltammetric, *in-situ* spectroelectrochemical, and *in-situ* electrocolorimetric responses of Lu(III) mono- and bis-phthalocyanines bearing 3,4-dimethoxyphenylthio substituents on peripheral and non-peripheral positions (Schemes 1 and 2). The results of this study

* Corresponding author. Tel.: +90 2163480292; fax: +90 2163480292.

E-mail addresses: erdogmusali@hotmail.com (A. Erdoğmuş), akoca@marmara.edu.tr (A. Koca).



Scheme 1. Synthetic route of 4-(3,4-(dimethoxy phenylthio))phthalonitrile (**1**) and its lutetium phthalocyanines (**4** and **5**).



Scheme 2. Synthetic route of 3-(3,4-(dimethoxy phenylthio))phthalonitrile (**3**) and 4,5-bis(3,4-(dimethoxyphenylthio))phthalonitrile (**2**) and their lutetium phthalocyanines (**6** and **7**).

will be used to decide possible technological applications of these novel complexes especially in electrochromic applications.

2. Synthesis

2.1. Materials

4-(3,4-(Dimethoxyphenylthio)) phthalonitrile (**1**), 4,5-bis[3,4-(dimethoxyphenylthio)]-phthalonitrile (**2**) and 3-(3,4-(dimethoxyphenylthio)) phthalonitrile (**3**) was synthesized according to procedures in the literatures [25–27]. *N,N'*-dimethylformamide (DMF), dimethyl sulfoxide (DMSO), chloroform (CHCl₃), tetrahydrofuran (THF), methanol (MetOH), dichloromethane (DCM), 1-pentanol, and n-hexane were purchased from Merck. 3-Nitrophthalonitrile, 4-nitrophthalonitrile, 4,5-dichlorophthalonitrile, 3,4-dimethoxythiophenol, tetrabutylammonium perchlorate (TBAP), 1,8-diazabicyclo[5.4.0]undec-7-ene (DBU), potassium carbonate, and lutetium(III) acetate were purchased from Aldrich. Column chromatography was performed on silica gel 60 (0.04–0.063).

2.2. Equipment

Absorption spectra were recorded on a Shimadzu 2001 UV spectrophotometer. FT-IR spectra were recorded on a Perkin Elmer Spectrum One Spectrometer using KBr. Mass spectra were acquired in the linear modes with average of 50 shots on a Bruker Daltonics Microflex mass spectrometer (Bremen, Germany) equipped with a nitrogen UV-Laser operating at 337 nm. 2 α -Cyano-4-hydroxycinnamic acid (20 mg/ml in THF) matrix for the complexes was prepared. MALDI samples were prepared by mixing compounds (2 mg/ml in THF) with the matrix solution (1:10, v/v) in a 0.5 ml eppendorf micro tube. Finally 1 μ l of this mixture was deposited on the sample plate, dried at room temperature and then analyzed.¹H NMR spectra were recorded on a Varian 500 MHz spectrometer in CDCl₃ solutions. Elemental analyses were performed using a Thermo flash EA 1112 Series. GC-MS spectra were acquired on a Agilent Technologies including 6890 N network GC system and 5973 inert Mass selective detector.

2.3. Synthesis

2.3.1. 2(3), 9(10), 16(17), 23(24)-Tetrakis-[3,4-(dimethoxyphenylthio)]phthalocyaninato lutetium(III) acetate (**4**) and bis-[27(24)-tetrakis-[3,4-(dimethoxy phenylthio)]phthalocyaninato]lutetium(III) (**5**)

A mixture of compound **1** (0.20 g, 0.68 mmol), lutetium(III) acetate (0.12 g, 0.34 mmol), and 2 ml of 1-pentanol were refluxed for 20 h in the presence of 1,8-diazabicyclo[5.4.0] undec-7-ene (DBU) (0.120 ml, 0.8 mmol) under the argon atmosphere. After cooling to the room temperature, the crude product was precipitated with n-hexane, collected by filtration, and then washed with hot hexane. The crude product was further purified by chromatography over a silica gel column using CHCl₃, a mixture of CHCl₃:THF (3:1 by volume) and a mixture of CHCl₃:THF:MetOH (3:1:10 by volume) as eluents, respectively. After the column chromatography, two products were obtained. For **4**, yield = 42 mg (15.97%). UV-vis in DCM (λ_{max} nm (log ε)): 354 (4.64), 628 (4.33), 695 (5.05). IR spectrum (cm⁻¹): 3055 (Ar-CH), 2992, 2929 (aliphatic-CH), 1728 (C=O), 1597, 1583, 1500 (C=C), 751 (C-S-C), 1436, 1392, 1319, 1250, 1229, 1176, 1134, 1072 (C-O-C), 1021, 907, 876, 804 (Pc skeleton). Elemental analyses data for C₆₆H₅₁N₈O₁₀S₄Lu: Required: C, 55.85; H, 3.62; N, 7.89; S, 9.04%. Found: C, 56.61; H, 3.70; N, 7.74; S, 9.11%. MS (ESI-MS) *m/z*: Calc.: 1419.4; Found: 1549.2 [M-Ac+ Cyano]⁺.

For **5**, yield = 26 mg (12%). UV-vis in DCM (λ_{max} nm (log ε)): 345 (4.91), 624 (4.40), 686 (4.98). IR spectrum (cm⁻¹): 3055 (Ar-CH),

2993, 2951, 2930 (aliphatic-CH), 1598, 1584, 1503 (C=C), 754 (C-S-C), 1438, 1396, 1313, 1253, 1230, 1177, 1135, (C-O-C), 1023, 907, 877, 806 (Pc skeleton). Elemental analyses data for C₁₂₈H₉₆N₁₆O₁₆S₈Lu: Required: C, 60.39; H, 3.80; N, 8.80; S, 10.08%. Found: C, 61.49; H, 3.71; N, 8.74; S, 10.28%. MS (ESI-MS) *m/z*: Calc.: 2545.7; Found: 2546.4 [M + H]⁺.

2.3.2. 2,3,9,10,16,17,23,24-Octakis-[3,4-(dimethoxyphenylthio)]phthalocyaninato lutetium(III) acetate (**6**)

The procedure for the synthesis of **6** was similar to that used for **4**, except compound **2** (0.32 g, 0.68 mmol) was used instead of compound **1**. The crude product was precipitated, collected by filtration and washed with hot hexane. Compound **6** was purified with column chromatography using a mixture of CHCl₃:THF (3:1 by volume) and CHCl₃:Methanol (1:1 by volume) as eluents. Compound **6** was obtained as a major product. Yield = 46 mg (12.74%). UV-vis in DCM (λ_{max} nm (log ε)): 358 (4.71), 639 (4.28), 708 (4.99). IR spectrum (cm⁻¹): 3055 (Ar-CH), 2951, 2931, 2833 (aliphatic-CH), 1583, 1501 (C=C), 1462, 1400, 1369, 1322, 1252 (C-O-C), 1023, 940, 876, 805 (Pc skeleton), 767, 753 (C-S-C). Elemental analyses data for C₆₄H₄₈N₈O₈S₄Lu: Required: C, 61.93; H, 3.90; N, 9.03; S, 10.33%. Found: 62.43; H, 4.00; N, 9.13; S, 10.20%. MS (ESI-MS) *m/z*: Calc.: 2092.2; Found: 2124.87 [M-Ac+ Cyano + 2H]⁺.

2.3.3. 1(4),10(13),19(22),28(31)-Tetrakis-[3,4-(dimethoxyphenylthio)]phthalocyaninato lutetium(III) acetate (**7**)

The synthesis of **7** was as outlined for **4**, except that compound **3** was used instead of the compound **1**. The crude product was precipitated, collected by filtration and washed with hot hexane. Compound **7** was purified with the column chromatography using a mixture of CHCl₃:THF (3:1 by volume) and CHCl₃:MetOH (1:1 by volume) as eluents. Yield = 130 mg (49.43%). UV-vis in DCM (λ_{max} nm (log ε)): 336 (4.61), 641 (4.28), 714 (4.98). IR spectrum (cm⁻¹): 3064, 2999 (Ar-CH), 2956, 2931, 2906 (aliphatic-CH), 1727 (C=O), 1584 (C=C), 1462, 1438, 1313, 1252, 1230 (C-O-C), 1022, 893, 876, 854 (Pc skeleton), 799, 748 (C-S-C). Elemental analyses data for C₆₆H₅₁N₈O₁₀S₄Lu: Required: C, 55.85; H, 3.62; N, 7.89; S, 9.04%. Found: C, 56.35; H, 3.72; N, 7.96; S, 8.94%. MS (ESI-MS) *m/z*: Calc.: 1419.4; Found: 1549.1 [M-Ac+ Cyano]⁺.

2.4. Electrochemical, *in-situ* spectroelectrochemical, and *in-situ* electrocolorimetric measurements

The electrochemical and spectroelectrochemical measurements were carried out with a Gamry Reference 600 potentiostat/galvanostat utilizing a three-electrode cell configuration at 25 °C. For cyclic voltammetry (CV), and square wave voltammetry (SWV) measurements, the working electrode was a Pt disc with a surface area of 0.071 cm². Surface of the working electrode was polished with a diamond suspension before each run. A Pt wire served as the counter electrode. Saturated calomel electrode (SCE) was employed as the reference electrode and separated from bulk of the solution by a double bridge. Ferrocene was used as an internal reference. Tetrabutylammonium perchlorate (TBAP) in dichloromethane (DCM) and/or dimethylsulfoxide (DMSO) was employed as the supporting electrolyte at a concentration of 0.10 mol dm⁻³. High purity N₂ was used to remove dissolved O₂ for at least 15 min prior to each run and to maintain a nitrogen blanket during the measurements. IR compensation was applied to the CV and SWV scans to minimize the potential control error.

UV/Vis absorption spectra and chromaticity diagrams were measured by an OceanOptics QE65000 diode array spectrophotometer. *In-situ* spectroelectrochemical measurements were carried out by utilizing a three-electrode configuration of a thin-layer

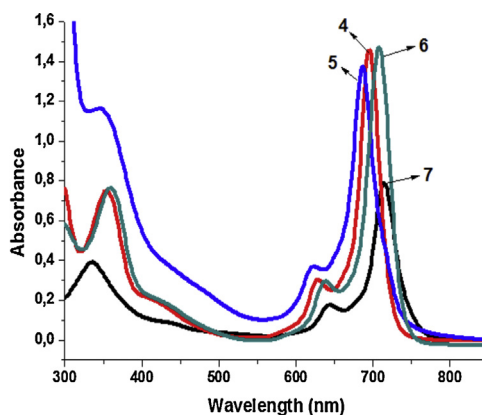


Fig. 1. UV-vis spectra of compounds **4–7** in DCM.

quartz spectroelectrochemical cell at 25 °C. The working electrode was a Pt semi-transparent electrode. A Pt wire counter electrode separated by a glass bridge and a SCE reference electrode separated from bulk of the solution by a double bridge were used.

In-situ electrocolorimetric measurements under potentiostatic control were obtained using an OceanOptics QE65000 diode array spectrophotometer at color measurement mode by utilizing three-electrode configuration of a thin-layer quartz spectroelectrochemical cell. The standard illuminant A with 2-degree observer at constant temperature in a light booth designed to exclude external light was used. Prior to each set of measurements, background color coordinates (x , y and z values) were taken at open-circuit, using the electrolyte solution without MPC under study. During the measurements, readings were taken as a function of time under kinetic control, however the color coordinates at the beginning and final of each redox processes were also reported.

3. Results and discussion

3.1. Synthesis and characterization

Schemes 1 and 2 show the synthetic route involved for the formation of the complexes **4–7**. The lutetium phthalocyanines (**4–7**) were formed by cyclotetramerization of the compounds **1**, **2** and **3** in the presence of anhydrous Lu(CH₃COO)₃. Purification of the complexes was achieved by column chromatography. The compounds **4–7** were soluble in THF, CHCl₃, DMF, and DMSO. Moreover, all compounds were soluble in methanol except the compound **5**.

FTIR, UV-vis, and mass spectroscopies, as well as elemental analysis performed the characterizations of lutetium phthalocyanines. All results of the complexes are consistent with the assigned formulations (**Schemes 1 and 2**). The characteristic vibrations corresponding to C≡N were observed at 2230 cm⁻¹, 2227 cm⁻¹ and 2231 cm⁻¹ for **1**, **2** and **3** in the FTIR spectra, respectively. The ether (C—O—C) and the thioether (C—S—C) vibrations for compounds **1**, **2** and **3** were observed at 1277 cm⁻¹ and 740 cm⁻¹, at 1253 cm⁻¹ and 762 cm⁻¹ and at 1023 cm⁻¹ and 729 cm⁻¹, respectively. The strong CN vibrations of **1–3** were disappeared after conversion to the complexes **4–7**. In the FTIR spectra of compounds **4–7**, weak bands observed above 3000 cm⁻¹ are due to the aromatic C—H stretching. The aliphatic C—H stretching vibrations of the synthesized complexes were observed between 2960 and 2850 cm⁻¹. In all complexes, the characteristic vibrations corresponding to the thioether groups (C—S—C) were observed at 751 nm (for **4**), 754 nm (for **5**), 753 nm (for **6**), and 748 nm (for **7**).

The best evidence for phthalocyanine systems are given by their UV-vis spectra in solution. The ground state electronic absorption spectra of the compounds **4–7** are given in **Fig. 1**. The UV-vis

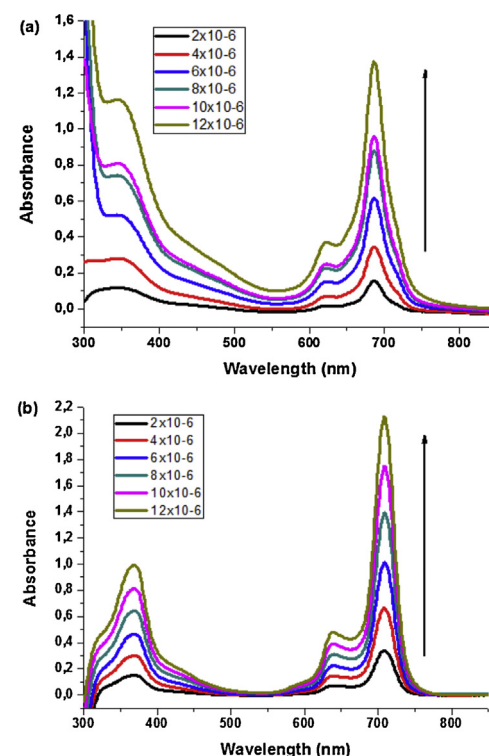


Fig. 2. Aggregation behaviours of **5** (a) in DCM and **7** (b) in DMSO at different concentrations: (2×10^{-6} to 12×10^{-6} mol dm⁻³).

absorption spectra of the compounds **4–7** indicate the characteristic intense Q bands at 695, 686, 708, and 714 nm, respectively. In addition, the intense B bands were observed at 354 nm for **4**, 345 nm for **5**, 358 nm for **6** and 336 nm for **7** (**Fig. 1**). For the metallophthalocyanine bearing thioether moieties on the non-periphery, the Q band is shifted to the longer wavelength as a result of the electron-donating ability of the thioether substituents as shown in **Fig. 1**. The aggregation behaviors of lutetium phthalocyanines (**4–7**) were also investigated at different concentration in DMSO. Aggregation is usually depicted as a coplanar association of rings progressing from monomer to dimer and higher order complexes [26]. As the concentration was increased, the intensity of absorption of the Q band also increased and there were no new bands (normally blue shifted) due to the aggregated species. Beer-Lambert law was obeyed for the complexes in DMSO in the concentration ranging from 2×10^{-6} to 10×10^{-6} mol dm⁻³ (**Fig. 2**) [26].

The mass spectra of **4–7** confirmed the proposed structures. The molecular ion peaks were observed at *m/z* 1549.2 (M-Ac + cyano) for **4** and **7**, 2546.4 (M + H) for **5** and 2124.87 (M-Ac + cyano + 2H) for **6**, respectively. Elemental analysis results were also consistent with the proposed structures of the synthesized phthalonitrile and phthalocyanine compounds (**1–7**).

3.2. Electrochemical measurements

Bis phthalocyanine complexes (LuPc₂) have a sandwich structure involving a metal center between two Pcs. However monomeric LuPc complexes include the same metal center at the outer space of Pcs ring due to the big size of metal center. The structural differences between the sandwich complex and the others are well reflected by their voltammetric behaviors [28]. Thus the voltammetric analyses of the newly synthesized **4–7** complexes were studied to clarify the effects of these structural differences to the electrochemical behavior of the complexes. Solvent effects to the electrochemistry of the complexes were also studied in DMSO

Table 1
Voltammetric data of the complexes.

Complex	$E_{1/2}$ vs. SCE ^b	Ring oxidations		Ring reductions			$\Delta E_{1/2}^a$
		O ₂	O ₁	R ₁	R ₂	R ₃	
LuPc (4) in DCM	$E_{1/2}$ vs. SCE ^b	1.16 ^c	0.66	-0.89	-1.33		
	ΔE_p (mV) vs. SCE ^d	-	62	62	80		1.55
	I_{pa}/I_{pc} ^e	-	0.98	0.91	0.23		
LuPc (6) in DCM	$E_{1/2}$ vs. SCE ^b	1.30	0.63	-0.94	-1.28	-1.52	
	ΔE_p (mV) ^d	120	55	80	57	-	1.57
	I_{pa}/I_{pc} ^e	-	0.84	0.85	0.90	-	
LuPc (7) in DCM	$E_{1/2}$ vs. SCE ^b	1.03	0.58	-0.98	-1.44 ^c		
	ΔE_p (mV) ^d	90	70	60	-		1.56
	I_{pa}/I_{pc} ^e	0.34	0.98	0.94	0.97		
LuPc (4) in DMSO	$E_{1/2}$ vs. SCE ^b		0.68	-0.80	-0.99	-1.26	-1.47
	ΔE_p (mV) ^d		60	-	-	-	148
	I_{pa}/I_{pc} ^e		0.87	-	-	-	
LuPc (6) in DMSO	$E_{1/2}$ vs. SCE ^b	-	0.65	-0.87	-1.01	-125	-1.46
	ΔE_p (mV) ^d	-	73	61	63	85	-
	I_{pa}/I_{pc} ^e	-	0.89	0.97	0.54	0.65	-
LuPc (7) in DMSO	$E_{1/2}$ vs. SCE ^b	1.13	0.62	-1.00	-1.11	-1.36	-1.57
	ΔE_p (mV) ^d	-	85	61	63	85	-
	I_{pa}/I_{pc} ^e	-	0.93	0.97	0.54	0.65	-
LuPc₂ (5) in DCM	$E_{1/2}$ vs. SCE ^b	1.11 ^c	0.52	0.14	-0.92	-1.21	-1.62
	ΔE_p (mV) ^d	-	63	59	65	73	75
	I_{pa}/I_{pc} ^e	-	0.96	1.00	0.87	0.85	-
LuPc₂ (5) in DMSO	$E_{1/2}$ vs. SCE ^b	-	0.63	0.27	-0.81	-1.10 (-1.30)	-1.59
	ΔE_p (mV) ^d	-	90	57	62	120	80
	I_{pa}/I_{pc} ^e	-	0.87	0.98	0.92	-	0.87

TW: This work.

^a $\Delta E_{1/2} = E_{1/2}$ (first oxidation) – $E_{1/2}$ (first reduction) = HOMO–LUMO gap.

^b $E_{1/2} = (E_{pa} + E_{pc})/2$ at 0.100 V s⁻¹.

^c The process is recorded with SWV.

^d $\Delta E_p = |E_{pa} - E_{pc}|$.

^e I_{pa}/I_{pc} for reduction, I_{pc}/I_{pa} for oxidation processes at 0.100 V s⁻¹ scan rate.

and DCM solvents. Table 1 lists the assignments of the redox couples and the electrochemical parameters, which included half-wave peak potentials ($E_{1/2}$), anodic to cathodic peak potential separation (ΔE_p), ratio of anodic to cathodic peak currents (I_{pa}/I_{pc}), and difference between the first oxidation and reduction potentials ($\Delta E_{1/2}$).

All electrochemical analyses were performed in both DCM (non-polar and noncoordinating solvent) and DMSO solvent media (polar and coordinating solvent) to investigate the effect of the solvent to the redox behavior of the complexes. As shown in Fig. 3, all mono LuPc complexes give very similar voltammetric responses in DCM/TBAP electrolyte system on a Pt working electrode with small potential shifts due to the different position and the number of the substituents. Mono LuPc complexes (**4**, **6**, and **7**) give two reduction and two oxidation couples. $\Delta E_{1/2}$ values of all mono LuPcs are between 1.48 and 162 V, which are in harmony with those of MPc having redox inactive metal center and mono LuPc complexes [29–32]. While the first reduction and the first oxidation couples of all monomeric LuPc complexes are electrochemically and chemically reversible, the second oxidation and reductions are irreversible with respect to ΔE_p and $I_{p,a}/I_{p,c}$ values [33]. Comparing ΔE_p values of them with those of ferrocene were also used to check the electrochemical reversibilities of the complexes. As shown from the figure, substituting the complex at the nonperipheral position (complex **7**) instead of the peripheral position (complex **4**) shifts the redox processes approximately 100 mV toward the negative potential. The reversibility of the complexes gets worse, when LuPc is substituted on nonperipheral position (complex **7**). The redox processes of octa substituted LuPc (**6**) shifts approximately 50 mV toward the negative potentials with respect to the peripheral tetra substituted LuPc (**4**) due to the presence of more electron releasing

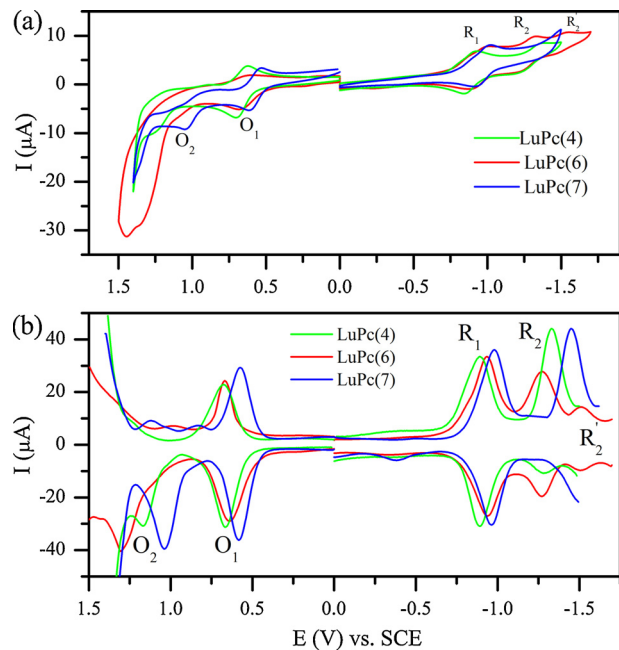


Fig. 3. (a) CVs of **4**, **6**, and **7** (5.0×10^{-4} mol dm⁻³) at 0.10 V s⁻¹ scan rate on Pt in DCM/TBAP. (b) SWVs of **4**, **6**, and **7**, SWV parameters: pulse size = 100 mV; Step Size: 5 mV; Frequency: 25 Hz.

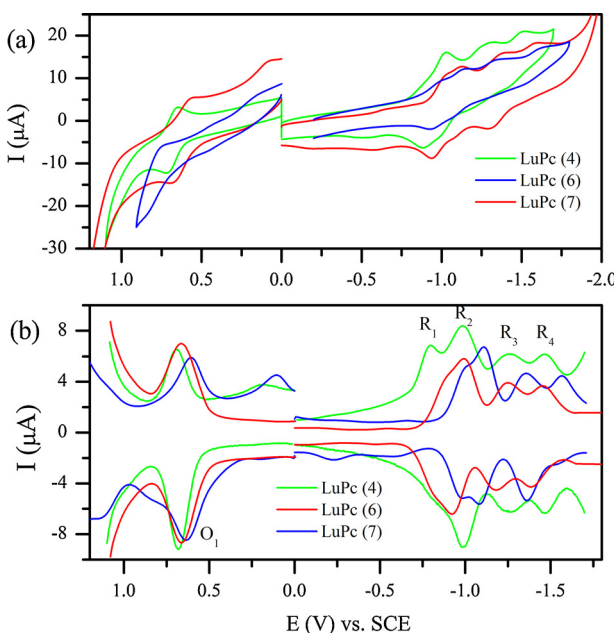


Fig. 4. (a) CVs of **4**, **6**, and **7** (5.0×10^{-4} mol dm⁻³) at 0.10 V s⁻¹ scan rate on Pt in DMSO/TBAP. (b) SWV of **4**, **6**, and **7**, SWV parameters: pulse size = 100 mV; Step Size: 5 mV; Frequency: 25 Hz.

dimethoxyphenylthio substituents on the complex **6**. Differently all redox processes of **6** are out of the reversible peak character.

When DMSO (polar and coordinating solvent) was used instead of DCM (nonpolar and noncoordinating solvent) as the solvent of the complexes, each reduction reaction of the complexes splits into two waves (Fig. 4). Thus, while these complexes give two reduction reactions in DCM, they give four reduction reactions in DMSO. Due to the splitting of the reduction reactions, peak analyses of the complexes (especially ΔE_p and $I_{p,a}/I_{p,c}$ values) could not be performed. Splitting of the reduction processes may be due to the coordination of DMSO to the lutetium center of the complexes. Coordinating of DMSO forms equilibrium between coordinated and non-coordinated complexes. Coordinated and non-coordinated complexes can transfer electrons at different potentials. Thus, DMSO splits the redox processes of the complexes. DCM is not a coordinating solvent, consequently the splitting behaviors of the complexes could not be observed in DCM. Coordinating effect of MPcs with different ligands is well documented in literature and our results are in agreement with the literature [30]. Another common difference between the redox behaviors of the complexes in different solvents is the shifting of the electron transfer processes to the negative potentials due to the higher polarizing effect of DMSO than DCM.

The redox properties of LuPc₂ complex (**5**) were studied and compared with those of the LuPc complexes. The complex **5** gives four reversible reduction processes, labeled as R₁ at 0.15 V, R₂ at -0.92 V, R₃ at -1.22 V, and R₄ at -1.62 V as well as one reversible and one irreversible oxidation processes, labeled as O₁ at 0.52 V and O₂ at 1.10 V in DCM/TBAP and these redox processes shift to negative potentials in DMSO/TBAP. Fig. 5 shows the CV and SWV of the complex in DCM/TBAP and DMSO/TBAP. Table 1 lists the fundamental electrochemical parameter of the complex. All redox processes are Pc ring-based, because lutetium metal center is redox inactive in Pc core [32]. The electrochemical processes are schematically illustrated in Scheme 3, where the reductions were labeled as R₁, R₂, R₃, and R₄ and the oxidations as O₁ and O₂. Scheme 4 shows the origin of these electron transfer reactions, which were indicated on the molecular orbital diagram of LuPc₂ [15]. As shown in Table 1 and Figs. 3–5, the redox potential of R₁ of **5** is shifted to the

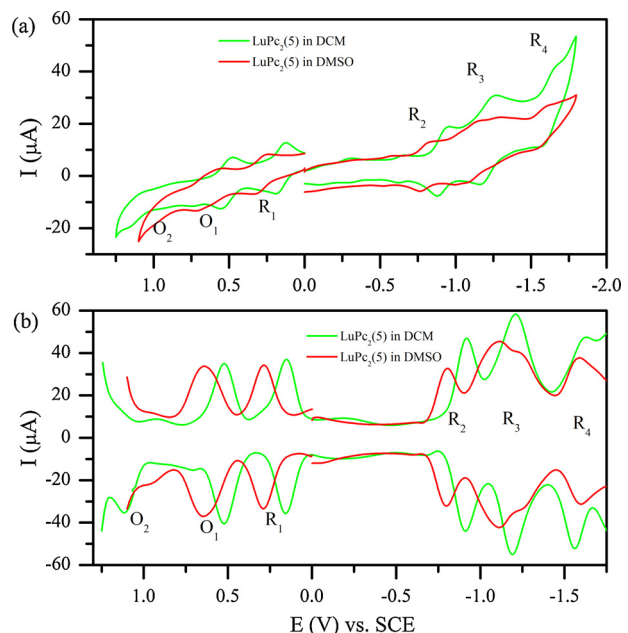
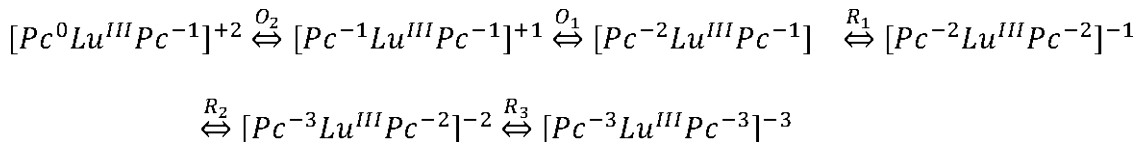


Fig. 5. (a) CVs and (b) SWV of **5** (5.0×10^{-4} mol dm⁻³) at 0.10 V s⁻¹ scan rate on Pt in DCM/TBAP and DMSO/TBAP electrolyte systems.

anodic side due to the radical form of the one Pc ring of the complex. While mono PCs give the first reduction process at around -0.90 V, the complex **5** gives the first reduction process at 0.14 V in DCM and 0.27 V in DMSO. On the other hand, the potential of O₁ for **5** is recorded at less positive potential than those of the mono Pc compounds. The $\Delta E_{1/2}$ value of **5** decreases to 0.38 V due to the shifting of peaks, while these values of the mono LuPcs are higher than 1.50 V. The value of $\Delta E_{1/2}$ reflects the energy separation between the SOMO and the LUMO of the bis-phthalocyanine neutral forms, and HOMO and LUMO for the mono LuPcs. In turn, the values of the potential R₂ were estimated to be similar for the R₁ of all the mono Pc complexes.

To investigate the effect of the solvent, CV and SWV of **5** were also recorded in DMSO/TBAP electrolyte system. When compared with the CV and SWV of **5** in DCM, it is clear that the redox processes of the complex interestingly shift to the positive potentials. Because redox processes generally shifts to the negative potentials in DMSO with respect to DCM due to the electron donating ability of the polar DMSO solvent. Another different behavior of the complex in DMSO is the splitting of the R₃ process. This extraordinary behavior is most probably due to the change the interaction of Pc rings of **5** as a result of the interaction with DMSO.

The number of transferred electrons for each redox process of the complexes was determined by CPC measurements at suitable constant peak potentials. Faraday law was used to derive the number of electron transferred during the electrolysis of the complex under constant potential applications. CPC showed that all redox processes of the complex are one-electron redox couples. CV, SWV and spectroelectrochemical measurements given below also support one-electron character of the redox couples. It is well known that peak current of a process is directly proportional with the 3/2 order of the transferred electrons. Thus it could be proposed the transferred electrons with comparing the peak current of the redox processes. Characteristic spectral changes during the in-situ spectroelectrochemical measurements of a complex could be also used to determine the transferred electron numbers. For instance, observation of the spectral changes (which are characteristic for monoanionic LuPc₂ species under 0.0 V potential application) indicated one-electron transfer feature of R₁ couple of LuPc₂.

**Scheme 3.** Redox mechanism of the complex 5.

3.3. Spectroelectrochemical studies

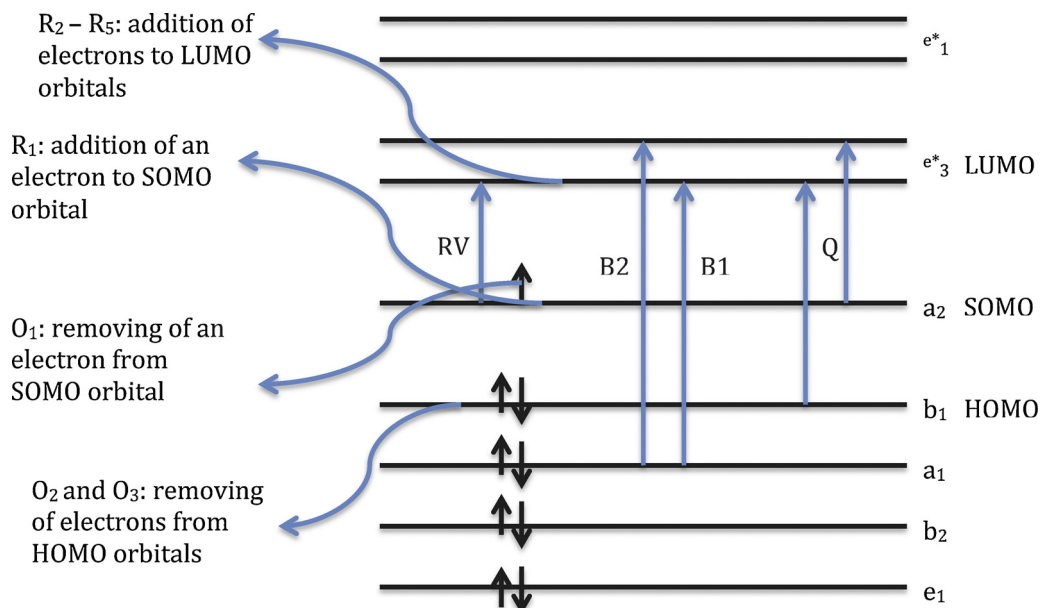
It is well known that lanthanide phthalocyanines, especially sandwich type phthalocyanine metal complexes reveal strong changes in their electronic absorption spectra from UV up to near-IR region while undergoing oxidation and reduction, and are thus promising electrochromic materials [34]. Thus spectroelectrochemical analyses of the complexes were performed to perform assignments of the redox processes and to determine the spectrum and color of the electrogenerated anionic and cationic form of the complexes.

All mono LuPc complexes give very similar spectral changes during the spectroelectrochemical measurements. While all mono LuPc complexes give distinct spectral changes in DMSO, the spectral changes in DCM are not easily discerned. The different in-situ spectroelectrochemical behaviors of the complexes in different solvent are in harmony with the voltammetric responses of the complexes in these solvents. Different behaviors of the complexes in DMSO and DCM were arisen from the different nature of these solvents. Coordinating and more polarizing nature of DMSO affects the voltammetric and spectroscopic behavior of the complexes more than these of noncoordinating DCM solvent.

Fig. 6 illustrates the UV/Vis spectral changes for the complex **4** in DMSO/TBAP during controlled-potential electrolysis, which reflect transformation of the neutral phthalocyanine into the electron-reduced and oxidized forms, respectively [35–37]. As shown in **Fig. 6a**, while the Q band at 697 nm decreases in intensity with slight shifting to 692 nm, a new band is recorded at 584 nm during the first reduction reaction. Moreover the B band at 361 nm decreases in intensity and a new band is observed at 434 nm. During this electrochemical reduction reaction, well recorded isosbestic points are observed at 385, 625, 635, and 721 nm, which demonstrates that reduction gives a single reduced product. The Q band

decreases without shifting during the Pc based reduction processes of the metallophthalocyanines bearing redox inactive metal center [26,28,38]. But differently the Q bands of mono LuPcs shift to the higher energy side during the Pc ring reduction process of the LuPcs. So we can easily assign this process to $[AcO-Lu^{III}Pc^{-2}]/[AcO-Lu^{III}Pc^{-3}]^{-1}$ reduction.

Fig. 6b illustrates the spectral changes during the second and third reduction processes. These spectral changes are also consistent with the second and third Pc based reduction processes of MPcs. Thus we assigned these processes to $[AcO-Lu^{III}Pc^{-3}]^{-1}/[AcO-Lu^{III}Pc^{-4}]^{-2}$ and $[AcO-Lu^{III}Pc^{-4}]^{-2}/[AcO-Lu^{III}Pc^{-5}]^{-3}$, respectively [5,36–39]. Spectral changes during the first oxidation process are given in **Fig. 6c**. As shown in this figure, the Q band decreases in intensity, while two new bands are recorded at 349 and 848 nm. These new bands are resulted from the metal to ligand charge transfer (MLCT) processes. These spectral changes are in agreement with the Pc based oxidation of the MPc complexes. All spectral changes of the complex are in agreement with the orbital diagrams of these types' complexes [15]. The color change of the complexes during the redox processes were recorded using *in-situ* colorimetric measurements. **Fig. 6d** shows the chromaticity diagrams of **4** recorded simultaneously during the spectroelectrochemical measurements. Without any potential application, the solution of **4** is green ($x=0.3033$ and $y=0.3657$). As the potential is stepped from 0 to -1.00 V , the color of neutral **4** starts to change and a light blue color ($x=0.2681$ and $y=0.3326$) of monoanionic form of the complex was obtained at the end of the first reduction. Similarly the color of the dianionic and trianionic species was recorded as deep blue and monocationic species has yellow color ($x=0.3558$ and $y=0.3353$). As shown in **Fig. 6d**, electrogenerated forms of the complex have distinct color changes, which are the desired properties of a material for electrochromic application. All color changes are reversible. Application of the potential of the previous process

**Scheme 4.** Origin of the electron transfer reactions on the molecular orbital diagram of LuPc₂ [15].

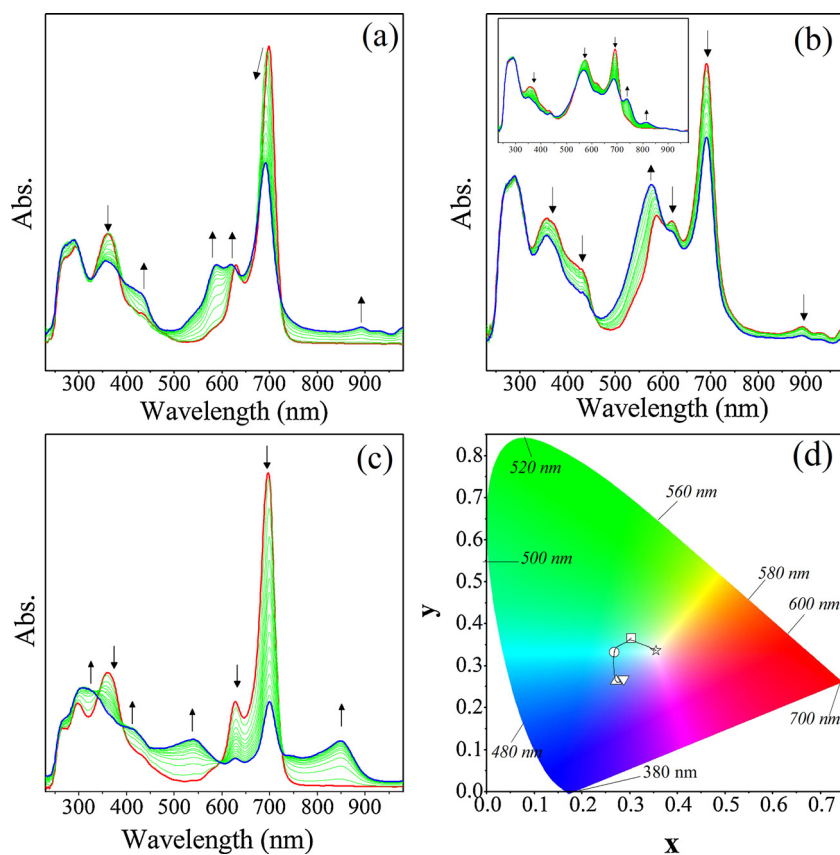


Fig. 6. *In-situ* UV-vis spectral changes of **4** in DMSO/TBAP. (a) $E_{app} = -1.10$ V. (b) $E_{app} = -1.30$ V (inset: $E_{app} = -1.50$ V). (c) $E_{app} = 0.80$ V. (d) Chromaticity diagram of **4**. Each symbol represents the color of electro-generated species; □: [AcO-Lu^{III}Pc⁻²], ○: [AcO-Lu^{III}Pc⁻³]⁻¹, ▲: [AcO-Lu^{III}Pc⁻³]⁻², ▼: [AcO-Lu^{III}Pc⁻⁴]⁻³, ☆: [AcO-Lu^{III}Pc¹]⁺¹.

immediately changed the color to the color of the previous species. Reversibility of the color changes were tested by applying different potentials to the working electrode. Approximately similar color coordinated were recorded during the repetitive switching of the redox processes.

As shown in Fig. 7, the complex **7** gives very similar spectral changes with the complex **4** during the spectroelectrochemical measurements in DMSO. While the Q band shifts from 715 nm to 675 nm, a new band is recorded at 608 nm during the first reduction process (Fig. 7a). Similarly the Q band at 675 nm decreases without shifting and a new MLCT band is recorded at 563 nm during the second reduction process (Fig. 7b). Fig. 7c illustrates the spectral changes during the oxidation processes. As shown in this figure, spectral changes which are consistent with the Pc based oxidation are recorded during the first oxidation process. The Q band decreases in intensity and two new MLCT bands are recorded at 800 and 882 nm during the first oxidation reaction. These spectroscopic changes indicate a Pc based oxidation process. The monocationic species decomposed during the second oxidation process as shown in Fig. 7c inset. Fig. 7d illustrates the distinct color differences between the electrogenerated anionic and cationic forms of the complex.

Spectroelectrochemical studies were employed to confirm the assignments in the CVs of the sandwich type complex **5**. The complex **5** shows different spectral changes in DMSO and in DCM solvents during reduction processes. Fig. 8 illustrates the *in-situ* UV-vis spectral changes of **5** in DCM during the redox processes. Spectral changes in the NIR region are characteristics for the **5** complexes. As Ishikawa and co-workers [39,40] reported the band at 940 nm is easily assigned to the nondegenerate HOMO–LUMO transition, which corresponds to the charge resonance HOMO–SOMO

excitation in the neutral form. During the oxidation and reduction of the neutral form of **5**, new bands appear near the former position of this band, which are characteristic changes for the sandwich type Pc complexes [15,39,40]. Under 0.0 V potential application, while the Q band at 688 nm decreases in intensity, a new Q band for the reduced species is recorded at 643 nm. The broad band at around 450 nm and the band at 940 nm, which are characteristic bands for the radical Pc ring, disappear during this process (Fig. 8a). These spectral changes are characteristic changes for the sandwich type Pc complexes and easily assigned to $[Pc^{-1}Lu^{III}Pc^{-2}] / [Pc^{-2}Lu^{III}Pc^{-2}]^{-1}$ redox reaction [39–41]. During this process, well-defined isosbestic points are recorded at 397, 568, 668, 705, and 765 nm, which demonstrate that the reduction proceeds cleanly in deoxygenated DCM to give a single reduced species. Green color of the neutral **5** ($x=0.3241$ and $y=0.3811$) changed to greenish blue ($x=0.2842$ and $y=0.3605$) at the end of the first reduction (Fig. 8d). When reverse potential was applied, the original green color was obtained reversibly. Fig. 8b illustrates *in-situ* UV-vis spectral changes of **5** during the second and third redox processes, which indicate the one-electron ring based reductions of the complex. Distinct spectral changes during these reduction processes also alter the color of the complex. While blue color ($x=0.2555$ and $y=0.3282$) is obtained at the end of the second reduction process, the blue color changes to purple ($x=0.2868$ and $y=0.2762$) at the end of the third reduction process (Fig. 8d). UV-vis spectra of the complex also change significantly during the oxidation processes (Fig. 8c). While the Q band shifts to 724 nm, the band at around 470 nm increases in intensity in addition to the enhanced band at 841 nm during the first oxidation process. These spectral changes indicate radical form of the both Pc rings of the sandwich type complex. Since the band at 470 nm characterizing radical form

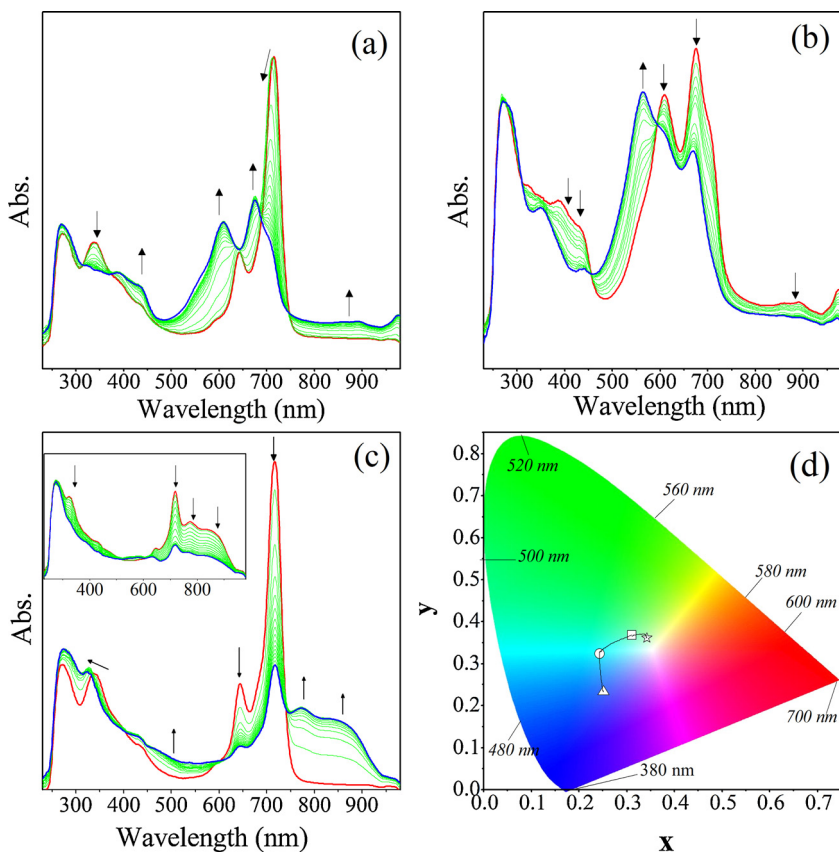


Fig. 7. *In-situ* UV-vis spectral changes of **7** in DMSO/TBAP. (a) $E_{app} = -1.10$ V. (b) $E_{app} = -1.30$ V. (c) $E_{app} = -0.70$ V (inset: $E_{app} = -1.30$ V). (d) Chromaticity diagram of **7**. Each symbol represents the color of electro-generated species; □: $[\text{AcO-Lu}^{\text{III}}\text{Pc}^{-2}]$, ○: $[\text{AcO-Lu}^{\text{III}}\text{Pc}^{-3}]^{-1}$, ▲: $[\text{AcO-Lu}^{\text{III}}\text{Pc}^{-3}]^{-2}$, ☆: $[\text{AcO-Lu}^{\text{III}}\text{Pc}^1]^{+1}$.

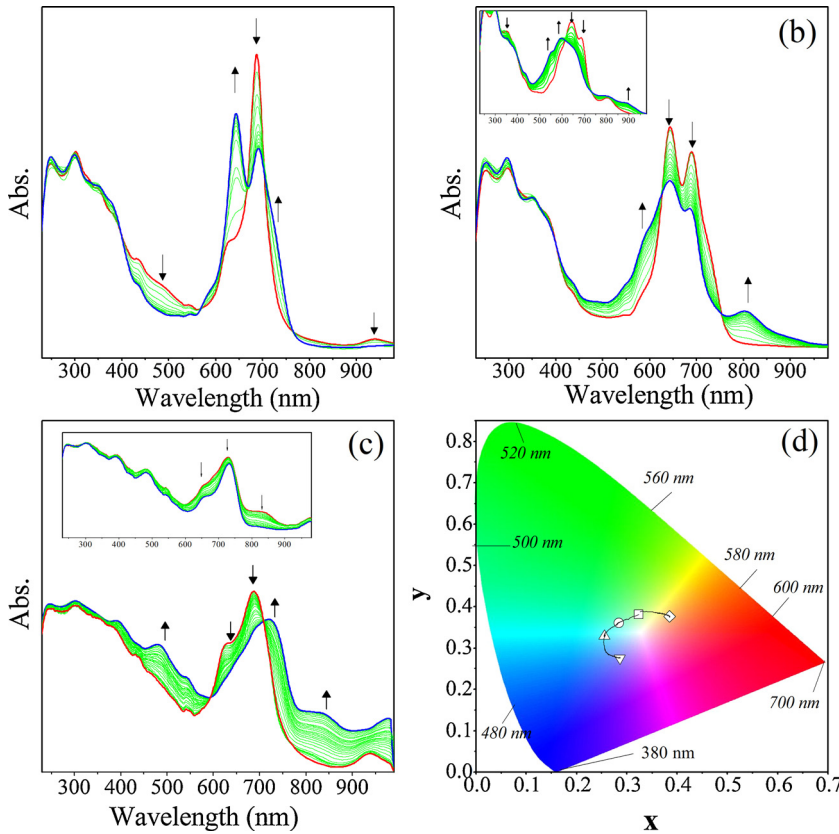


Fig. 8. *In-situ* UV-vis spectral changes of **5** in DCM/TBAP. (a) $E_{app} = 0.00$ V. (b) $E_{app} = -1.00$ V (inset: $E_{app} = -1.30$ V). (c) $E_{app} = 0.60$ V (inset: $E_{app} = 1.30$ V). (d) Chromaticity diagram of **5**. Each symbol represents the color of electro-generated species; □: $[\text{Pc}^{-1}\text{Lu}^{\text{III}}\text{Pc}^{-2}]$, ○: $[\text{Pc}^{-2}\text{Lu}^{\text{III}}\text{Pc}^{-2}]^{-1}$, ▲: $[\text{Pc}^{-3}\text{Lu}^{\text{III}}\text{Pc}^{-2}]^{-2}$, ▼: $[\text{Pc}^{-3}\text{Lu}^{\text{III}}\text{Pc}^{-3}]^{-3}$, ☆: $[\text{Pc}^{-1}\text{Lu}^{\text{III}}\text{Pc}^{-1}]^{+1}$.

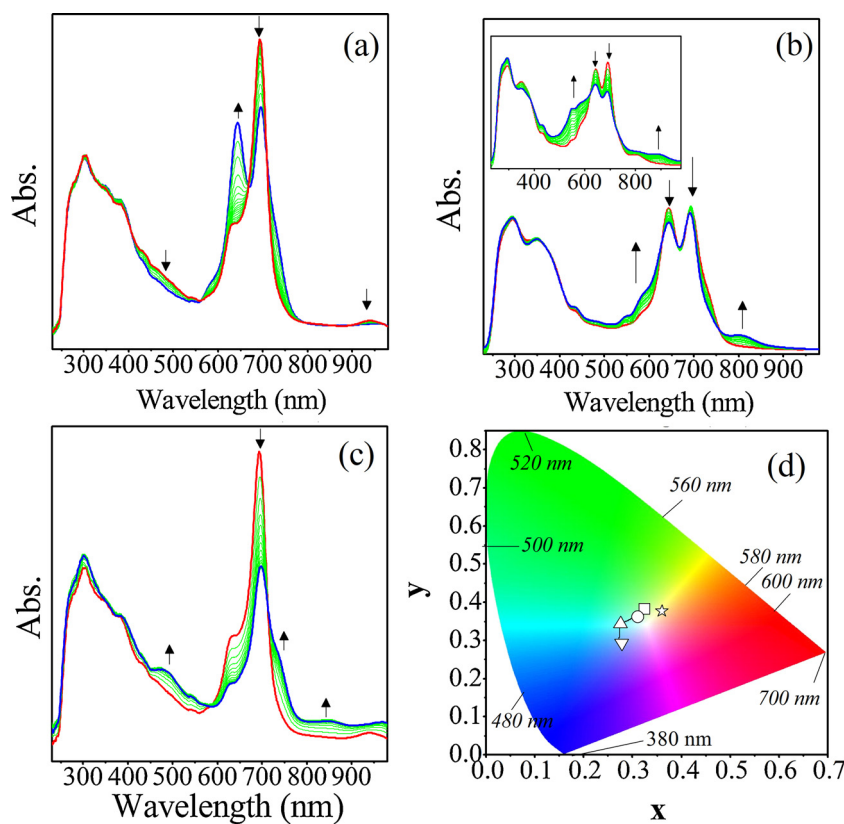


Fig. 9. *In-situ* UV-vis spectral changes of **5** in DMSO/TBAP. (a) $E_{app} = 0.00$ V. (b) $E_{app} = -1.00$ V (inset: $E_{app} = -1.20$ V. (c) $E_{app} = 0.70$ V. (d) Chromaticity diagram of **5**. Each symbol represents the color of electro-generated species; □: $[Pc^{-1}Lu^{III}Pc^{-2}]^-$, ○: $[Pc^{-2}Lu^{III}Pc^{-2}]^{-1}$, △: $[Pc^{-3}Lu^{III}Pc^{-2}]^{-2}$, ▽: $[Pc^{-3}Lu^{III}Pc^{-3}]^{-3}$, ☆: $[Pc^{-1}Lu^{III}Pc^{-1}]^1$.

of the one **Pc** ring of the complex increases in intensity. All bands decrease in intensity due to the decomposition of the complex during the second oxidation process as shown in Fig. 8c inset. Color of the monocationic species was recorded as yellow ($x = 0.3854$ and $y = 0.376$) as shown in Fig. 8d. Measurement of the xyz coordinates allows quantification of each color of redox species that is very important to decide their possible electrochromic application.

Fig. 9 illustrates the *in-situ* UV-vis spectral changes of **5** in DMSO. The complex **5** gives very similar spectroscopic changes during the redox processes in both of DCM and DMSO. During the first reduction process at 0.0 V, while the Q band at 695 nm decreases in intensity a new band is recorded at 645 nm. At the same time, the bands at 480 and 943 nm, which characterize the radical neutral **5**, disappear completely (Fig. 9a). During this process, well-defined isosbestic points are recorded at 405, 560, 668, and 710 nm. Yellowish green color of the neutral **5** ($x = 0.3244$ and $y = 0.383$) changed to light green ($x = 0.3105$ and $y = 0.362$) at the end of the first reduction (Fig. 9d). General trend of the spectral changes during the further reductions and oxidation processes of the complex in DMSO are very similar with those in DCM with little change differences as shown in Fig. 9. Distinct color change of the complex during the redox processes were recorded using *in-situ* colorimetric measurements. Fig. 9d gives the chromaticity diagrams of **5** recorded simultaneously during the spectroelectrochemical measurements. Measurement of the xyz coordinates of the complex and distinct differences between the different redox states of the complex indicate possible electrochromic application of the complex in both DCM and DMSO solvent media.

4. Conclusions

Voltammetric and spectroelectrochemical studies show that mono lutetium phthalocyanine complexes gave ring-based,

multi-electron and reversible/quasi-reversible redox processes. The peak potentials of the redox processes were affected considerably from the position and the number of the substituent. Solvent of the electrolyte also affected the redox behavior of the complexes. The first reduction process recorded at around 0.14 V is characteristics for the reduction of the radical **Pc** ring of the sandwich phthalocyanine. Definite determination of the colors of the electro-generated anionic and cationic form of the complexes is important to decide the possible electrochromic application of the complexes. Multiple electron transfer reactions at small potentials, reversible and diffusion controlled character of these processes and the distinct color differences between the electrogenerated anionic and cationic forms of the complexes are the desired properties for the usage of a material in the most of the electrochemical technologies such as electrosensor, electrocatalytic, and display applications. In our forthcoming studies electrochromic application of these complexes will be performed.

Acknowledgments

This work is supported by TUBITAK (Project no: 111T179) and Yildiz Technical University (Project No: 2012-01-02-KAP03).

Appendix A. Supplementary data

Supplementary data associated with this article can be found, in the online version, at <http://dx.doi.org/10.1016/j.electacta.2013.09.088>.

References

- [1] T. Basova, A.G. Gurek, V. Ahsen, A. Ray, Electrochromic lutetium phthalocyanine films for *in situ* detection of NADH, *Opt. Mater.* 35 (2013) 634.

- [2] H. Yamamoto, Y., Ushioda, M., Tanaka, S., Yamaguchi, H. Enjoji, A multicolor electrochromic display using phthalocyanine films with solid electrolyte, Proc. 6th Int. Disp. Conf. SID, Tokyo, 1986, p. 94.
- [3] M.M. Nicholson, F.A. Pizzarello, Cathodic electrochromism of lutetium diphthalocyanine films, *J. Electrochem. Soc.* 128 (1981) 1740.
- [4] P. Petit, P. Turek, J.J. Andre, R. Even, J. Simon, R. Madru, M. Alsadoun, G. Guillaud, M. Maitrot, Molecular semiconductors: phthalocyanine radicals. Magnetic and electrical properties, field effect transistors, *Synth. Met.* 29 (1989) 59.
- [5] R.B. Lu, K.S. Xu, Z.K. Zhang, J.H. Zhong, G.Z. Li, H.M. Wu, Z.H. Lu, Nematic liquid crystal alignment on phthalocyanine LB films, *Mol. Cryst. Liq. Cryst. A* 289 (1996) 77.
- [6] X. Zuo, H. Zhang, N. Li, An electrochemical biosensor for determination of ascorbic acid by cobalt(II) phthalocyanine–multi-walled carbon nanotubes modified glassy carbon electrode, *Sensor Actuat. B-Chem.* 161 (2012) 1074.
- [7] B. Ceken, M. Kandaz, A. Koca, Electrochemical metal-ion sensors based on a novel manganese phthalocyanine complex, *Synth. Met.* 162 (2012) 1524.
- [8] B. Ceken, M. Kandaz, A. Koca, Electrochemical hydrogen peroxide sensor based on cobalt phthalocyanine captured in polyaniline film on a glassy carbon electrode, *J. Porphyr. Phthalocya.* 16 (2012) 380.
- [9] W.J.R. Santos, A.L. Sousa, R.C.S. Luz, F.S. Damos, L.T. Kubota, A.A. Tanaka, S.M.C.N. Tanaka, Amperometric sensor for nitrite using a glassy carbon electrode modified with alternating layers of iron(III) tetra-(N-methyl-4-pyridyl)-porphyrin and cobalt(II) tetrasulfonated phthalocyanine, *Talanta* 70 (2006) 588.
- [10] A. Koca, A. Kalkan, Z.A. Bayir, Electrocatalytic oxygen reduction and hydrogen evolution reactions on phthalocyanine modified electrodes: electrochemical, in situ spectroelectrochemical, and in situ electrocolorimetric monitoring, *Electrochim. Acta* 56 (2011) 5513.
- [11] T. Mugadza, T. Nyokong, Synthesis, characterization and the electrocatalytic behaviour of nickel (II) tetraamino-phthalocyanine chemically linked to single walled carbon nanotubes, *Electrochim. Acta* 55 (2010) 6049.
- [12] P. Mashazi, E. Antunes, T. Nyokong, Probing electrochemical and electrocatalytic properties of cobalt(II) and manganese(III) octakis(hexylthio)phthalocyanine as self-assembled monolayers, *J. Porphyr. Phthalocya.* 14 (2010) 932.
- [13] R.D. Gould, Structure and electrical conduction properties of phthalocyanine thin films, *Coord. Chem. Rev.* 156 (1996) 237.
- [14] S.V. Kudrevich, J.E. vanLier, Azaanalogs of phthalocyanine: syntheses and properties, *Coord. Chem. Rev.* 156 (1996) 163.
- [15] A.B.P.L.C.C. Leznoff, Phthalocyanines, Properties and Applications, 4th ed., Wiley-VCH, 1996.
- [16] V.I. Gavrilov, A.P. Konstantinov, E.A. Lukyanets, I.V. Shelepin, Electrochromism of solid films of the blue form of lutetium phthalocyanine, Sov. Eletrochem. Engl. Transl. 22 (1986) 1562.
- [17] D.J. Zhang, F.L. Lu, H.C. Huang, J. Wang, H. Yu, J.Z. Jiang, D.H. Yan, Z.Y. Wang, Near infrared electrochromism of lutetium phthalocyanine, *Synth. Met.* 148 (2005) 123.
- [18] Y.Q. Liu, K. Shigehara, A. Yamada, Purification of lutetium diphthalocyanine and electrochromism of its Langmuir–Blodgett films, *Thin Solid Films* 179 (1989) 303.
- [19] C. Pal, A.K. Ray, R. Withnall, Study of electrochromic behaviour of bis octakis(octyl)phthalocyanato lutetium(III) and detection of biomolecules *in situ*, in: XXII International Conference on Raman Spectroscopy, vol. 1267, 2010, p. 611.
- [20] M.L. Rodriguez-Mendez, R. Aroca, J.A. Desaja, Electrochromic and gas adsorption properties of Langmuir–Blodgett films of lutetium bisphthalocyanine complexes, *Chem. Mater.* 5 (1993) 933.
- [21] F. Castaneda, V. Pllichon, Electrochemical process in electrochromic films of lutetium diphthalocyanine, *J. Electroanal. Chem.* 236 (1987) 163.
- [22] M.T. Riou, M. Auregan, C. Clarisse, Electrochromic properties of lutetium diphthalocyanine films, *J. Electroanal. Chem.* 187 (1985) 349.
- [23] D. Wohrle, M. Eskes, K. Shigehara, A. Yamada, A simple synthesis of 4,5-disubstituted 1, 2-dicyanobenzenes and 2, 3, 9, 10, 16, 17, 23, 24-octasubstituted phthalocyanines, *Synthesis-Stuttgart* (1993) 194.
- [24] A.G. Gurek, O. Bekaroglu, Octakis (alkylthio)-substituted phthalocyanines and their interactions with silver (I) and palladium (II) ions, *J. Chem. Soc. Dalton Trans.* (1994) 1419.
- [25] D. Arıcan, M. Arıcı, A.L. Uğur, A. Erdoğmuş, A. Koca, Effects of peripheral and nonperipheral substitution to the spectroscopic, electrochemical and spectroelectrochemical properties of metallophthalocyanines, *Electrochim. Acta* 106 (2013) 541.
- [26] C. Öztürk, A. Erdoğmuş, M. Durmuş, A.L. Uğur, F.A. Kılıçarslan, I. Erden, Highly soluble 3,4-(dimethoxyphenylthio) substituted phthalocyanines: synthesis, photophysical and photochemical studies, *Spectrochim. Acta A* 86 (2012) 423.
- [27] M. Arıcı, D. Arıcan, A.L. Uğur, A. Erdoğmuş, A. Koca, Electrochemical and spectroelectrochemical characterization of newly synthesized manganese, cobalt, iron and copper phthalocyanines, *Electrochim. Acta* 87 (2013) 554.
- [28] V.E. Pushkarev, A.Y. Tolbin, F.E. Zhurkin, N.E. Borisova, S.A. Trashin, L.G. Tomilova, N.S. Zefirov, Sandwich double-decker lanthanide (III)intracavity complexes based on clamshell-type phthalocyanine ligands: synthesis, spectral, electrochemical, and spectroelectrochemical investigations, *Chem-Eur. J.* 18 (2012) 9046.
- [29] A. Koca, A.R. Ozkaya, M. Selcukoglu, E. Hamuryudan, Electrochemical and spectroelectrochemical characterization of the phthalocyanines with pentafluorobenzoyl substituents, *Electrochim. Acta* 52 (2007) 2683.
- [30] A.B.P. Lever, E. Milaeva, The redox chemistry of metallophthalocyanines in solution, in: C.C. Leznoff (Ed.), *The Phthalocyanines, Properties and Applications*, vol. 2, Wiley, 1992, p. 162.
- [31] M. Ozer, A. Altindal, A.R. Ozkaya, M. Bulut, O. Bekaroglu, Synthesis, characterization and some properties of novel bis (pentafluorophenyl) methoxyl substituted metal free and metallophthalocyanines, *Polyhedron* 25 (2006) 3593.
- [32] P. Sen, F. Dumludağ, B. Salih, A.R. Ozkaya, O. Bekaroglu, Synthesis and electrochemical, electrochromic and electrical properties of novel s-triazine bridged trinuclear Zn (II), Cu (II) and Lu (III) and a tris double-decker Lu (III) phthalocyanines, *Synth. Met.* 161 (2011) 1245.
- [33] W.R.H. Peter Kissinger, *Laboratory Techniques in Electroanalytical Chemistry*, 2nd ed., Marcel Dekker, New York, 1996.
- [34] R.J.M. Paul, M.S. Monk, David R. Rosseinsky, *Electrochromism: Fundamentals and Applications*, Wiley-VCH Verlag GmbH, 2007.
- [35] I.V. Zhukov, V.E. Pushkarev, L.G. Tomilova, N.S. Zefirov, Correlations between electrochemical and spectral properties of alkyl-substituted diphthalocyanine lanthanide complexes, *Russ. Chem. B+* 54 (2005) 189.
- [36] I. Yilmaz, T. Nakanishi, A. Gurek, K.M. Kadish, Electrochemical and spectroscopic investigation of neutral, oxidized and reduced double-decker lutetium (III) phthalocyanines, *J. Porphyr. Phthalocya.* 7 (2003) 227.
- [37] Y.Q. Liu, K., Shigehara, M., Hara, A., Yamada, Electrochemistry and electrochromic behavior of langmuir–blodgett films of octakis-substituted rare-earth meta1 diphthalocyanines, *J. Am. Chem. Soc.* 113 (1991) 440.
- [38] D. Quinton, E. Antunes, S. Griveau, T. Nyokong, F. Bediouï, Cyclic voltammetry and spectroelectrochemistry of a novel manganese phthalocyanine substituted with hexynyl groups, *Inorg. Chem. Commun.* 14 (2011) 330.
- [39] N. Ishikawa, Y. Kaizu, Axially polarized NIR absorption bands in electron-deficient lanthanide phthalocyanine dimers and trimers, *J. Porphyr. Phthalocya.* 3 (1999) 514.
- [40] N. Ishikawa, Electronic structures and spectral properties of double-and triple-decker phthalocyanine complexes in a localized molecular orbital view, *J. Porphyr. Phthalocya.* 5 (2001) 87.
- [41] C. Apetrei, S. Casilli, M. De Luca, L. Valli, J. Jiang, M.L. Rodriguez-Mendez, J.A. De Saja, Spectroelectrochemical characterisation of Langmuir–Schaefer films of heteroleptic phthalocyanine complexes. Potential applications, *Colloid Surf. A* 284 (2006) 574.